

Optical characteristics of strontium barium niobate thin films depending on temperature

© K.M. Zhidel¹, A.V. Pavlenko^{1,2}

¹ Scientific Research Institute of Physics, Southern Federal University, Rostov-on-Don, Russia

² Southern Scientific Center, Russian Academy of Sciences, Rostov-on-Don, Russia

e-mail: karinagidele@gmail.com

Received October 24, 2024

Revised October 24, 2024

Accepted March 22, 2025

The optical properties of single-crystal thin films of $\text{Sr}_{0.61}\text{Ba}_{0.39}\text{Nb}_2\text{O}_6$, with a thickness of ~ 646 nm, synthesized on MgO (001) substrates using high-frequency cathode sputtering in an oxygen atmosphere, have been studied using spectrophotometry in the spectral range 200–1000 nm and at temperatures between 299.15–393.15 K. It has been observed that the edge of the optical absorption in the transmission spectra of the $\text{Sr}_{0.61}\text{Ba}_{0.39}\text{Nb}_2\text{O}_6/\text{MgO}$ system shifts towards the long-wavelength region with increasing temperature. The dispersion dependences of the refractive index $n(\lambda)$ and extinction coefficient $k(\lambda)$ of the film have been calculated at fixed temperatures. It has been shown that the film has slightly lower values of these optical parameters compared to the single-crystal $\text{Sr}_{0.61}\text{Ba}_{0.39}\text{Nb}_2\text{O}_6$ material. The dispersion of $n(\lambda)$ has been interpreted within the framework of the individual dipole oscillator model and approximated using the Cauchy relation. The results obtained in this study indicate the stability of the optical properties of $\text{Sr}_{0.61}\text{Ba}_{0.39}\text{Nb}_2\text{O}_6$ heterostructures grown on MgO substrates over a given wavelength range within the specified temperature range.

Keywords: thin films, strontium barium niobate, SBN, transmission spectrum, absorption edge, Urbach energy, band gap.

DOI: 10.61011/EOS.2025.04.61408.7251-24

Introduction

Strontium barium niobate ($\text{Sr}_x\text{Ba}_{1-x}\text{Nb}_2\text{O}_6$, SBN) is an environmentally friendly lead-free uniaxial relaxor ferroelectric crystal with the tetragonal tungsten bronze structure. SBN single crystals [1–5] are of great fundamental and applied research interest, since they have high potential for practical use in modern microelectronic and optoelectronic devices [4,6]. The refinement of deposition techniques has made it possible to obtain heterostructures based on high-quality SBN thin films [7]. When incorporated into optoelectronic devices [6], such structures are better suited to the industrial needs than their bulk counterparts due to the potential for fabrication of integrated devices and control over the properties of thin films in accordance with specific requirements. New applications of ferroelectric materials in modern photonic devices have also been explored in recent years [8]. It is evident that the temperature dependence of the refraction index is of particular importance for photonic devices, since a number of optical phenomena, design, and operational characteristics depend on it. It is known that the refraction indices of the most common photonic semiconductors (Si or GaAs) increase with temperature [9]. During operation, a certain fraction of supplied power is inevitably dissipated as heat, which leads to an increase in temperature of the crystal lattice and, consequently, a change in refraction index, exerting a negative influence on the device performance parameters. An understanding of thermo-optical properties is key to monitoring and controlling temperature-induced changes in parameters [10].

Thus, data on the thermo-optical characteristics of strontium barium niobate thin films are of critical importance for future applications in the development of new devices.

In the present study, we report the results of examination of the spectral dependence of transmittance of single-layer SBN-61 heterostructures on MgO (001) substrates obtained by RF cathode sputtering in oxygen at high temperatures $t = 299.15\text{--}393.15$ K and $\lambda = 200\text{--}1000$ nm.

Objects. Fabrication and research methods

Single-crystal $\text{Sr}_{0.61}\text{Ba}_{0.39}\text{Nb}_2\text{O}_6$ films were formed by gas-discharge RF cathode sputtering on 0.5-mm-thick single-crystal (001) MgO substrates (polished on both sides). Deposition was performed at the „Plasma 50-SE“ setup (shared research facility of the Scientific Research Institute of Physics of the Southern Federal University) and followed the method detailed in [11]. The initial substrate temperature (before switching on the discharge) was ~ 673 K; after the discharge was switched on, the temperature was set within the range of 793–813 K. The pressure of pure oxygen in the chamber was maintained at 0.5 Torr throughout the entire process of sputtering, the RF power was 110 W, and the target–substrate distance was 12 mm.

Measurements of the spectral dependence of transmittance T of objects at wavelengths $\lambda = 200\text{--}1000$ nm were carried out using a complex based on an SF-56 UV spectrophotometer („OKB Spekt“, Russia) and an

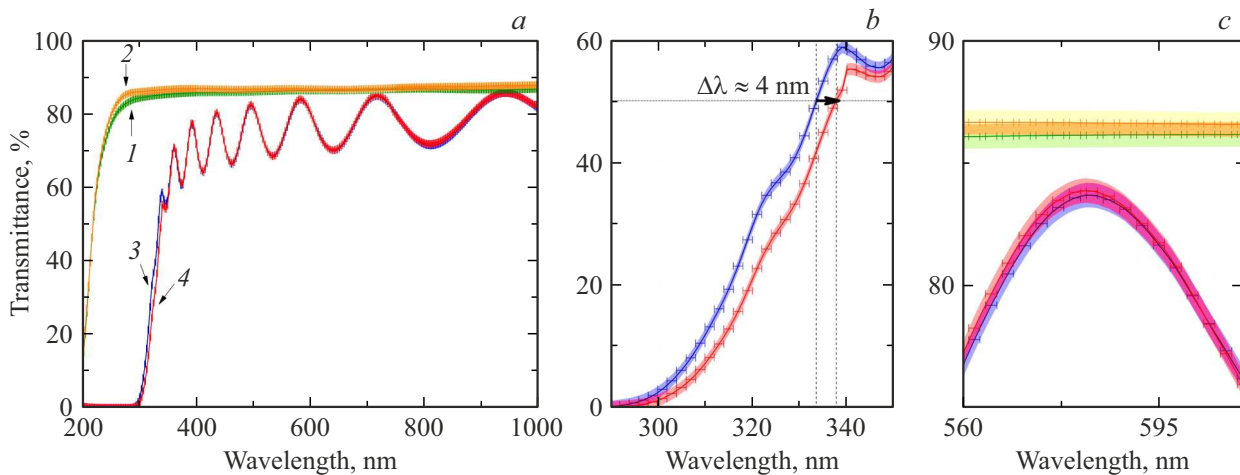


Figure 1. Transmittance spectra $T(\lambda)$: (a) 1, 2 — MgO substrate, 3, 4 — SBN-61/MgO heterostructure at $t = 299.15$ K and 393.15 K, respectively; (b) SBN-61/MgO optical absorption edge region; (c) zoomed-in spectral region.

LN-121-SPECTR cryostat („Kriogennye pribory,“ Russia) in the regime of heating from room temperature (RT, $t = 299.15$ K) to 393.15 K in vacuum. The scanning pitch was 1 nm.

Experimental results and discussion

Optical transmittance spectra $T(\lambda, t)$ of the SBN-61/MgO heterostructure and the MgO substrate recorded at fixed temperatures (RT and 393.15 K) are shown in Fig. 1, a.

SBN-61 films on MgO substrates are highly transparent ($T = 64\text{--}85\%$) in the visible and near IR spectral ranges. Compared to the MgO substrate transmittance (86% at RT), the optical transmittance of SBN-61/MgO is indicative of a smooth surface and fine film uniformity. Interference effects are also seen in the $T(\lambda)$ dependences for SBN-61/MgO. It is evident that the optical transmittance of SBN-61/MgO and the substrate itself changes slightly as the temperature increases. Notably, the transmittance spectra of SBN-61/MgO reveal a considerable shift of the optical absorption edge (Fig. 1, b) toward longer wavelengths at higher temperatures. This is indicative of a corresponding change in the optical constants and the optical band gap. It should be noted that the transmittance spectra are presented with the limits of absolute errors of measurement of T within the given spectral range and adjustment of wavelengths λ (Figs. 1, a–c). The shift of the optical absorption edge ($\Delta\lambda$) was estimated at a material transmittance level of 50% . It follows from the figure that we obtained the values of $\lambda_1 = 334$ nm at RT, $\lambda_2 = 338$ nm at 393.15 K, and $\Delta\lambda \sim 4$ nm (~ 0.05 eV).

A model of the „isotropic film/transparent substrate“ optical system with radiation incident normally to the film plane was used to process the transmittance spectra. Optical constants (refraction index n and extinction coefficient k) and thickness d were calculated by the envelope curve method [12,13] in the transparency region. To verify the

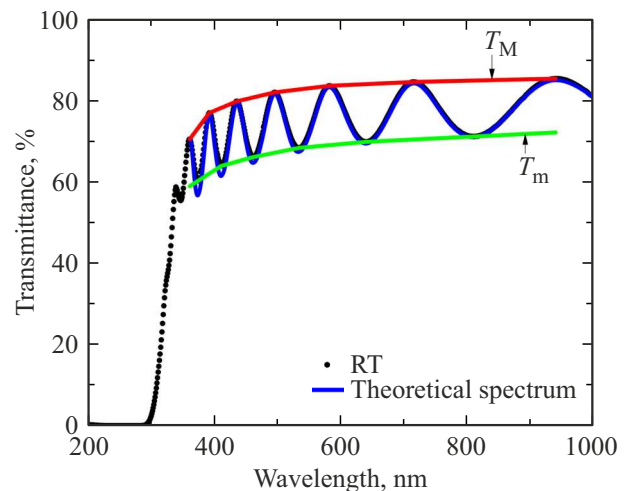


Figure 2. Transmittance spectra $T(\lambda)$ of SBN-61/MgO with envelope curves (T_M , T_m) and the theoretical spectrum at RT.

obtained values, theoretical transmittance spectra (Fig. 2) were modeled at constant temperatures. The theoretical spectra match the experimental ones, confirming the reliability of the obtained data. The spectrum at RT is shown as an example.

Figure 3 presents the dispersion dependences of optical constants of the SBN-61 film. Dependences $n(\lambda)$ and $k(\lambda)$ make it clear that the dispersion behavior of the curves is normal. Experimental $n(\lambda)$ and $k(\lambda)$ data are approximated well by Cauchy relations of the form

$$n(\lambda) = A + B/\lambda^2 + C/\lambda^4 + D/\lambda^6,$$

$$k(\lambda) = E + F/\lambda^2 + G/\lambda^4 + H/\lambda^6, \quad (1)$$

where λ is the wavelength and A , B , C , D , E , F , G , H are empirical constants.

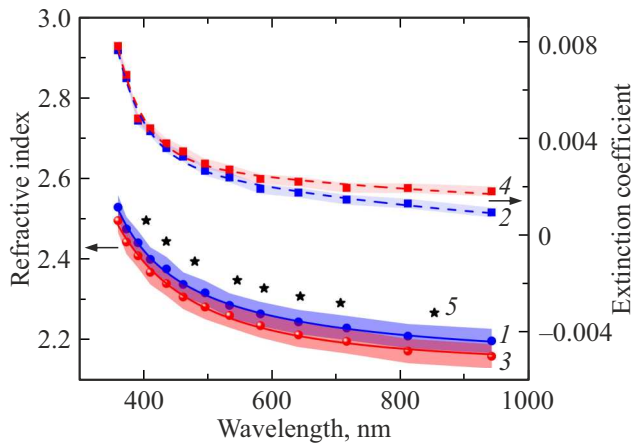


Figure 3. Wavelength dependences of refraction indices and extinction coefficients for the SBN-61 film at constant temperatures. Solid and dashed lines indicate the results of approximation with the Cauchy formula for $n(\lambda)$ (1, 3) and $k(\lambda)$ (2, 4), respectively; 5 — n_o of the SBN-61 single crystal [14]

The results of approximation with Cauchy relations are presented in Fig. 3. The Cauchy coefficients are listed in Table 1.

A comparison of the obtained data at RT with the values of ordinary refraction index (n_o) of the SBN-61 single crystal [14] at 297.65 K (see Fig. 3) reveals that the films have a slightly lower n within the studied wavelength range. It should be noted that n decreases further with an increase in temperature, but this reduction is within the permissible absolute error limit.

The refraction index reduction may be attributed to porosity and/or stress and strain in the films. Using the Lorentz–Lorenz model, one may define packing density P of a film as

$$P = [(n_f^2 - 1)(n_b^2 + 2)^{-1}] / [(n_b^2 - 1)(n_b^2 + 2)^{-1}], \quad (2)$$

where n_f — refraction index of the film and n_b — refraction index of the single crystal [14]. Setting $n_b = 2.4443$ (at 435.83 nm), we find that $P = 0.974$ for the SBN-61 film. This result illustrates the advantages of the used method for synthesis of films with given optical properties.

The refraction index dispersion data were also interpreted using the individual dipole oscillator model (the DiDomenico–Wemple model [15]). According to this model, the refraction index in the region of low absorption should follow relation

$$n^2(E) = 1 + E_d E_0 / (E_0^2 - E^2), \quad (3)$$

where E_d is the dispersion energy and E_0 is the oscillator energy.

The dependences of $1/(n^2 - 1)$ on $E^2(1/\lambda^2)$ (Fig. 4) were used to calculate the values of E_d and E_0 . Specifically, the oscillator energy was $E_0 = 6.129$ eV at RT and $E_0 = 6.054$ eV at 393.15 K, which is comparable with

literature data for other materials [16]. The dispersion energies are 22.33 eV and 21.18 eV, respectively.

The absorption spectra were analyzed in order to determine the magnitude and nature of the optical band gap. Absorption coefficient α in the region of strong absorption by the film material was calculated from the transmittance spectra in the following way [17]:

$$\alpha(\lambda) = 1/d \ln[(1 - R_1)(1 - R_2)(1 - R_{12})/T], \quad (4)$$

where d — film thickness and R_1 , R_2 , and R_{12} — coefficients of reflection from the air/film, film/substrate, and substrate/air interfaces, respectively.

As is known, the exponential absorption edge may be interpreted as a result of exponential distribution of local states in the band gap that is associated with the structure of materials. The Urbach rule [18] is valid in region $E < E_g$:

$$\alpha = \alpha_0 \exp[E_U(E - E_0)], \quad (5)$$

where E_U is the localized state tail width and α_0 is a constant corresponding to the absorption coefficient in the energy gap. Urbach energy E_U provides information regarding the existence of localized states in the band gap region. Their presence is associated with unsaturated bonds and/or defects in films and the degree of electron–phonon interaction. Thus, Urbach energy E_U is a measure of disorder in the system [18]. The value of E_U is estimated from the slope of the linear part of the $\ln \alpha(E)$ curve (see Fig. 5). The calculated Urbach energy values are presented in Table 2. The Urbach energy of SBN-61 films is ~ 0.216 eV at RT and increases with temperature (~ 0.242 eV), which suggests that the degree of structure ordering decreases.

According to the Tauc model [19], the transition type (direct or indirect) may be determined by plotting the dependences of $(\alpha h\nu)^m$ on E . Index of power $m = 2$ corresponds to an allowed direct transition, while $m = 1/2$

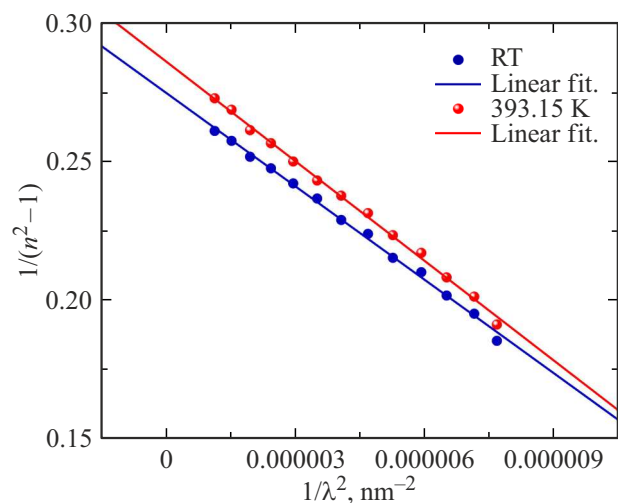


Figure 4. Dependences of $1/(n^2 - 1)$ on $1/\lambda^2$ plotted for the SBN-61 film at constant temperatures. Lines correspond to the results of approximation.

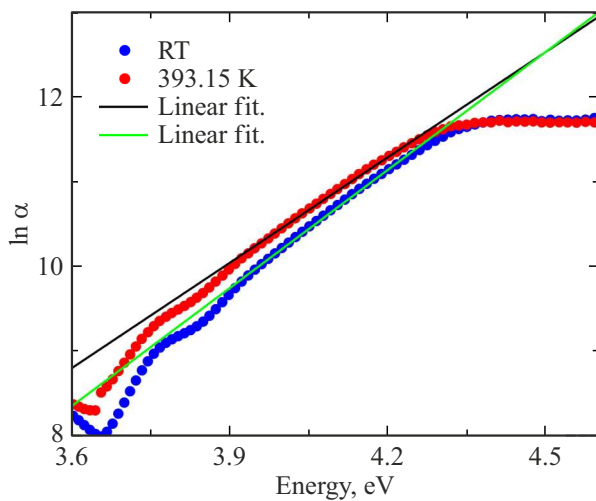
Table 1. Cauchy coefficients for $n(\lambda)$ and $k(\lambda)$ of the SBN-61 film

A		$B \cdot 10^4, \text{nm}^2$		$C \cdot 10^9, \text{nm}^4$		$D \cdot 10^{14}, \text{nm}^6$		$E \cdot 10^{-4}$		$F \cdot 10^3, \text{nm}^2$		$G \cdot 10^8, \text{nm}^4$		$H \cdot 10^{13}, \text{nm}^6$	
1*	2*	1	2	1	2	1	2	1	2	1	2	1	2	1	2
2.1496	2.1336	4.5136	2.5605	-3.096	2.6370	4.6645	1	-3.9757	7.9124	1.490	1.078	-3.2182	-2.675	3.434	3.1932

*1 — RT; 2 — 393.15 K.

Table 2. Optical characteristics of the SBN-61 film

d, nm	$E_g^{\text{dir}}, \text{eV}$			$E_g^{\text{ind}}, \text{eV}$			$E_{\text{ph}}, \text{meV} (\text{cm}^{-1})$			E_U, meV		
	RT	295 K [27]	393.15 K	RT	295 K [27]	393.15 K	RT	295 K [27]	393.15 K	RT	295 K [27]	393.15 K
646±30	4.121 ±0.004	4.28 [27]	4.066 ±0.005	3.628 ±0.003	3.67 [27]	3.573.15 ±0.003	47 (375)	105 (847) [27]	43 (345)	216	250 [27]	242


Figure 5. Calculation of the Urbach energy for SBN-61 films at constant temperatures. Lines correspond to the results of approximation.

corresponds to an allowed indirect one. A direct transition yields one linear section, and its extrapolation to the E axis provides the direct band gap value (E_g^{dir}). An indirect transition yields two linear sections leading to two extrapolations ($E_{g1} + E_{\text{ph}}$) and ($E_{g2} - E_{\text{ph}}$), where E_{ph} is the phonon energy facilitating the transition; E_{g1} is the absorption threshold corresponding to the process of phonon absorption; and E_{g2} is the absorption threshold corresponding to the process of phonon emission [20].

We have found that absorption coefficient α of the film in the region of intrinsic absorption is characterized well by the $(ah\nu)^2$ and $(ah\nu)^{1/2}$ dependences. This indicates that SBN-61 films have a direct- and indirect-type band gap in the region of higher and low energies, respectively. The results of approximation are listed in Table 2 and presented in Fig. 6. The coefficient of determination (R^2) was 0.99 for

all approximations. For clarity, the dependence of $(ah\nu)^{1/2}$ on E is plotted at RT only.

It follows from the data in Table 2 that the E_{ph} contribution decreases with increasing temperature. Naturally, films are characterized by a lower phonon energy E_{ph} than a single crystal. The E_{ph} value of our SBN-61 films (Table 2) is 43–47 meV, which corresponds to characteristic phonon frequencies of $\sim 345\text{--}375 \text{ cm}^{-1}$. According to the results of experimental Raman studies of ceramics [21], single crystals [22–25], and thin films of strontium barium niobate [26], these values are close to the frequencies of phonon modes that the authors associate with Nb–O stretching and O–Nb–O strain due to internal vibrations of NbO_6 octahedra [21–26]. As was noted in [21], an abrupt shift of line frequencies in the Raman spectra toward the low-frequency region at temperatures above 380 K is indicative of a phase transition (PT).

Having compared our results with the data for the SBN-61 single crystal [27], we conclude that the obtained SBN-61 films have optical band gaps that are quite close in magnitude under the assumption of direct and indirect transition types at RT. As the temperature increases, the E_g^{dir} and E_g^{ind} values for SBN-61 films decrease. Since pressure p and temperature t affect the crystal lattice parameters, their detectable influence on band gap E_g of the material was reported in [28,29]. The following relation characterizes the overall effect quantitatively:

$$\frac{dE_g}{dt} = \left(\frac{dE_g}{dt} \right)_v + \frac{\beta}{\gamma} \left(\frac{dE_g}{dp} \right)_t, \quad (6)$$

where β is the thermal expansion coefficient and γ is the compressibility. The typical magnitude of variation of E_g is $\approx -4 \cdot 10^{-4} \text{ eV per 1 K}$. Since all measurements in the present study were performed under vacuum conditions (i.e., at the same pressure), the variation of E_g with pressure is neglected. Our preliminary estimate of variation is $dE_g/dt \approx -0.0005 \text{ eV/K}^{-1}$ in the region from RT to 393.15 K.

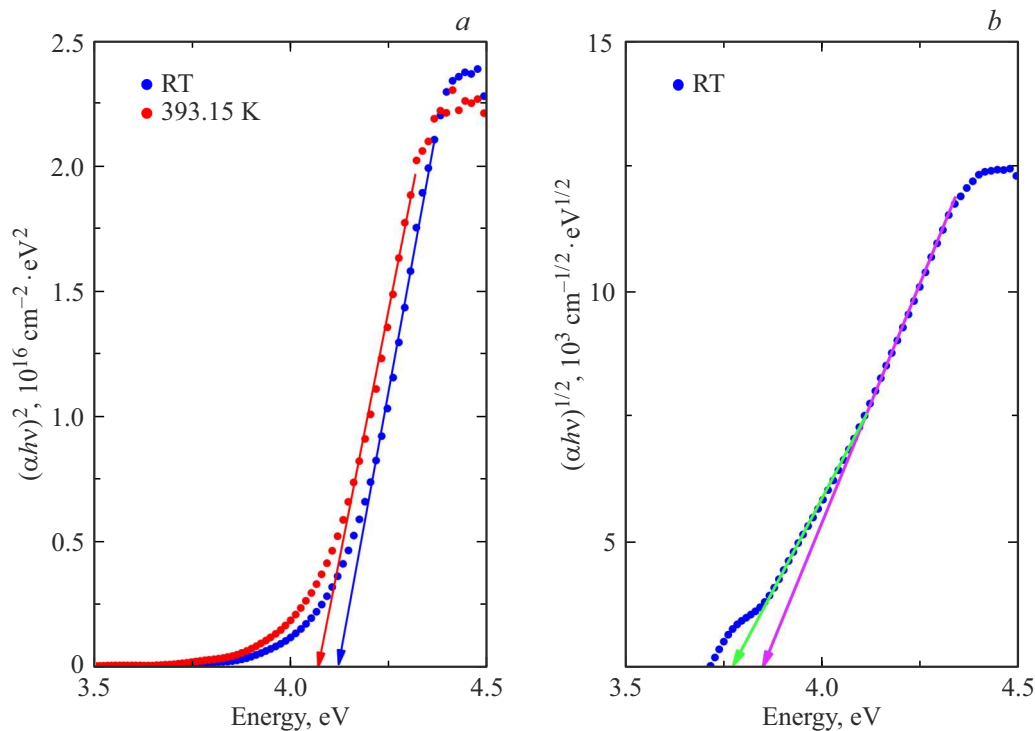


Figure 6. Dependences $(\alpha h\nu)^2$, $(\alpha h\nu)^{1/2}$ vs. E plotted for the SBN-61 film, which illustrate direct and indirect types of transition through the band gap.

The value of E_g may decrease due to an increase in amplitude of thermal vibrations of crystal lattice atoms and a change in interatomic distances during thermal expansion of the crystal. According to [30], where the behavior of lattice parameters of the $\text{Sr}_{0.61}\text{Ba}_{0.39}\text{Nb}_2\text{O}_6$ single crystal was characterized, the thermal motion of Nb atoms in the direction perpendicular to bond O–Nb–O leads to shortening of the O–O distance along axis c , which, in turn, results in negative thermal expansion. The values of parameter c start to decrease at t from 200 to 400 K and increase again above 400 K. It was also demonstrated that structural changes associated with the PT ($T_c \approx 350$ K) into the paraelectric phase start to manifest themselves at $t = 200$ K. Since it is fairly difficult to account rigorously for the factors mentioned above, dependence $E_g(t)$ is determined empirically, which will be the aim of our future studies.

Findings and conclusion

The results of an experimental spectrophotometric study of optical transmittance of the SBN-61/MgO (001) heterostructure within the temperature range of 299.15–393.15 K and the wavelength range of 200–1000 nm were reported. It was found that the optical absorption edge in the transmittance spectra of SBN-61/MgO shifts toward longer wavelengths at higher temperatures. At RT, the film material has $n = 2.38 \pm 0.03$ at $\lambda = 436$ nm, which is only slightly lower than n of

the SBN-61 single crystal ($n_b = 2.4443$). The dispersion dependences of refraction indices $n(\lambda)$ and extinction coefficients $k(\lambda)$ and the values of band gap determined as function of temperature under the assumption of direct E_g^{dir} and indirect E_g^{ind} allowed transitions for the SBN-61 film were presented. It was demonstrated that the refraction index dispersion may be interpreted within the individual oscillator model. The degree of ordering of the structure was estimated by approximating the absorption edge with an exponential dependence. The results revealed that the optical characteristics of SBN-61 thin films remain fairly stable within the examined temperature and wavelength ranges.

Funding

This study was supported financially by the Ministry of Science and Higher Education of the Russian Federation (state research assignment, project No. FENW-2023-0010/GZ0110/23-11-IF).

Acknowledgments

Equipment provided by the „Joint Scientific and Technological Equipment Center of the Southern Scientific Center of the Russian Academy of Sciences (Research, Development, Testing)“ shared research facility was used in the study.

Conflict of interest

The authors declare that they have no conflict of interest.

References

- [1] T. Lukaszewicz, M.A. Swirkowicz, J. Dec, W. Hofman, W. Szyrski. *J. Cryst. Growth*, **310** (7), 1464 (2008). DOI: 10.1016/j.jcrysgro.2007.11.233
- [2] M.D. Ewbank, R.R. Neurgaonkar, W.K. Cory, J. Feinberg. *J. Appl. Phys.*, **62** (2), 374 (1987). DOI: 10.1063/1.339807
- [3] P.V. Lenzo, E.G. Spencer, A.A. Ballman. *Appl. Phys. Lett.*, **11** (1), 23 (1967). DOI: 10.1063/1.1754944
- [4] R.R. Neurgaonkar, W.K. Cory, J.R. Oliver. *Ferroelectrics*, **51** (1), 3 (1983). DOI: 10.1080/00150198308009045
- [5] A.M. Glass. *J. Appl. Phys.*, **40** (12), 4699 (1969). DOI: 10.1063/1.1657277
- [6] S. Gupta, A. Paliwal, V. Gupta, M. Tomar. *Opt. Laser Technol.*, **122**, 105880 (2020). DOI: 10.1016/j.optlastec.2019.105880
- [7] D.V. Stryukov, Ya.Yu. Matyash, A.V. Pavlenko. *Fiz. Tverd. Tela*, **65** (11), 1964 (2023). DOI: 10.61011/0000000000 [D.V. Stryukov, Y.Y. Matyash, A.V. Pavlenko. *Phys. Solid State*, **65** (11), 1881 (2023). DOI: 10.61011/EOS.2025.04.61408.7251-24].
- [8] V.V. Krutov, A.S. Sigov, A.A. Shchuka. *Russ. Tekhnol. Zh.*, **5** (2), 3 (2017) (in Russian).
- [9] M. Han, and A. Wang. *Opt. Lett.*, **32** (13), 1800 (2007). DOI: 10.1364/OL.32.001800
- [10] E.D. Palik. *Handbook of Optical Constants of Solids* (Academic Press, Burlington, 1997).
- [11] A.V. Pavlenko, D.V. Stryukov, L.I. Ivleva, A.P. Kovtun, K.M. Zhidel, P.A. Lykov. *Phys. Solid State*, **63**, 286 (2021). DOI: 10.1134/S1063783421020219
- [12] R. Swanepoel. *J. Phys. E*, **16** (12), 1214 (1983). DOI: 10.1088/0022-3735/16/12/023
- [13] J.C. Manifacier, J. Gasiot, J.P. Fillard. *J. Phys. E*, **9** (11), 1002 (1976). DOI: 10.1088/0022-3735/9/11/032
- [14] Th. Woike, T. Granzow, U. Dörfler, Ch. Poetsch, M. Wöhlecke, R. Pankrath. *Phys. Status Solidi (A)*, **186** (1), R13 (2001). DOI: 10.1002/1521-396X(200107)186:1%3CR13::AID-PSSA999913%3E3.0.CO;2-G
- [15] S.H. Wemple, M. DiDomenico. *Phys. Rev. B*, **3** (4), 1338 (1971). DOI: 10.1103/PhysRevB.3.1338
- [16] Yu.S. Kuz'minov. *Segnetoelektricheskie kristally dlya upravleniya lazernym izlucheniem* (Nauka, M., 1982) (in Russian).
- [17] Yu.I. Ukhanov. *Opticheskie svoistva poluprovodnikov* (Nauka, M., 1977) (in Russian).
- [18] F. Urbach. *Phys. Rev.*, **92** (5), 1324 (1953). DOI: 10.1103/PhysRev.92.1324
- [19] J. Tauc, R. Grigorovici, A. Vancu. *Phys. Status Solidi (B)*, **15** (2), 627 (1966). DOI: 10.1002/pssb.19660150224
- [20] J. Sol?, L. Bausa, D. Jaque. *An Introduction to the Optical Spectroscopy of Inorganic Solids* (John Wiley & Sons, 2005).
- [21] Ya.Yu. Matyash, A.S. Anokhin, A.V. Pavlenko. *Phys. Solid State*, **11**, 1617 (2022). DOI: 10.61011/EOS.2025.04.61408.7251-24
- [22] K. Samanta, A.K. Arora, T.R. Ravindran, S. Ganesamoorthy, K. Kitamura, S. Takekawa. *Vib. Spectrosc.*, **62**, 273 (2012). DOI: 10.1016/j.vibspec.2012.07.002
- [23] R.E. Wilde. *J. Raman Spectrosc.*, **22** (6), 321 (1991). DOI: 10.1002/jrs.1250220604
- [24] K.G. Bartlett, L.S. Wall. *J. Appl. Phys.*, **44** (11), 5192 (1973). DOI: 10.1063/1.1662124
- [25] E. Amzallag, T.S. Chang, R.H. Pantell, R.S. Feigelson. *J. Appl. Phys.*, **42** (8), 3254 (1971). DOI: 10.1063/1.1660719
- [26] S. Gupta, A. Kumar, V. Gupta, M. Tomar. *Vacuum*, **160**, 434 (2019). DOI: 10.1016/j.vacuum.2018.11.057
- [27] K. Dorywalski, B. Andriyevsky, C. Cobet, M. Piasecki, I.V. Kityk, N. Esser, T. Łukasiewicz, A. Patryn. *Opt. Mater.*, **35** (5), 887 (2013). DOI: 10.1016/j.optmat.2012.10.050
- [28] F. Abeles. *Optical Properties of Solids* (North-Holland Publishing Company, Amsterdam and London, 1972).
- [29] D.L. Greenaway, G. Harbeke. *Optical Properties and Band Structure of Semiconductors* (Pergamon, 1968).
- [30] J. Schefer, D. Schaniel, V. Pomjakushin, U. Stuhr, V. Petříček, Th. Woike, M. Wöhlecke, M. Imlau. *Phys. Rev. B*, **74** (13), 134103 (2006). DOI: 10.1103/PhysRevB.74.134103

Translated by D.Safin